Helimagnetic Structure and Heavy-Fermion-Like Behavior in the Vicinity of the Quantum Critical Point in Mn_3P

Hisashi Kotegawa,[1] Masaaki Matsuda,[2] Feng Ye,[2] Yuki Tani,[1] Kohei Uda,[1] Yoshiki Kuwata,[1] Hideki Tou,[1] Eiichi Matsuoka,[1] Hitoshi Sugawara,[1] Takahiro Sakurai,[3] Hitoshi Ohta,[1,4] Hisatomo Harima,[1] Keiki Takeda,[5] Junichi Hayashi,[5] Shingo Araki,[6] and Tatsuo C. Kobayashi[6]

[1]*Department of Physics, Kobe University, Kobe 658-8530, Japan*
[2]*Neutron Scattering Division, Oak Ridge National Laboratory, Oak Ridge, Tennessee 37831, USA*
[3]*Research Facility Center for Science and Technology, Kobe University, Kobe, Hyogo 657-8501, Japan*
[4]*Molecular Photoscience Research Center, Kobe University, Kobe, Hyogo 657-8501, Japan*
[5]*Muroran Institute of Technology, Muroran, Hokkaido 050-8585, Japan*
[6]*Department of Physics, Okayama University, Okayama 700-8530, Japan*

(Received 15 July 2019; accepted 27 January 2020; published 25 February 2020)

Antiferromagnet Mn_3P with Neel temperature $T_N = 30$ K is composed of Mn tetrahedrons and zigzag chains formed by three inequivalent Mn sites. Due to the nearly frustrated lattice with many short Mn-Mn bonds, competition of the exchange interactions is expected. We here investigate the magnetic structure and physical properties including pressure effect in single crystals of this material, and reveal a complex yet well-ordered helimagnetic structure. The itinerant character of this materials is strong, and the ordered state with small magnetic moments is easily suppressed under pressure, exhibiting a quantum critical point at ~1.6 GPa. The remarkable mass renormalization, even in the ordered state, and an incoherent-coherent crossover in the low-temperature region, characterize an unusual electronic state in Mn_3P, which is most likely effected by the underlying frustration effect.

DOI: 10.1103/PhysRevLett.124.087202

The properties of interacting conduction electrons deviate from those of free electrons. Such interactions often result in the renormalization of the electron mass, which is the essence in strongly correlated electron systems. They are generally remarkable near an instability, such as itinerant-localized crossover like the Kondo effect, the proximity of a Mott insulator, and criticality of some degrees of freedom. Rich physics has been developed in such backgrounds including their interplay, and quantum criticality has been enthusiastically investigated for its ability to induce peculiar behaviors of electrons [1–4].

Magnetic frustration is also an important factor to induce a wide variety of physical phenomena. It can arise from geometrical constraint or from the competition of various short-range exchange interactions. The effect is generally not well established in itinerant magnetic systems, because it is thought to be weakened by long-range interactions. In itinerant systems, an aspect brought by competition of exchange interactions is a stabilization of helical magnetic structure, as has long been discussed in systems such as MnP-type materials [5–8]. Additionally, in such systems, the Dzyaloshinsky-Moriya (DM) interaction is often effective. It is also short-range exchange interaction, and contribution to the detailed helical structure has been suggested in MnP [9]. The competing exchange interactions and the DM interaction are characterized by crystal symmetry, general to many materials, and are the key inducers of rich and intriguing phenomena [10–12]. However, their role in the itinerant regime is poorly understood and remains an intriguing issue. Particularly, an interplay of the frustration and quantum phase transition has not been sufficiently explored in *d*-electron systems.

Expecting a remarkable frustration effect and an induced quantum phase transition, we spotlighted Mn_3P, whose properties have not been investigated sufficiently so far. An earlier study of polycrystalline samples had suggested an antiferromagnetic (AF) transition at $T_N = 115$ K [13], but a recent report has corrected this result to $T_N = 30$ K [14]. In the later paper, the Mössbauer spectroscopy and neutron diffraction measurements on slightly Fe-substituted samples suggested an ordered moment below 1 μ_B, indicating a remarkable itineracy of the Mn 3*d* electrons. However, the details of the magnetic structure are unknown [14].

Mn_3P crystallizes in a noncentrosymmetric tetragonal structure in the $I\bar{4}$ space group (No. 82, S_4^2) [15]. The crystal structure comprises three inequivalent Mn sites and one P site [see Fig. 1(a)]. The four Mn1 sites, denoted as $\alpha - \delta$ in Fig. 1, are equivalent and form a tetrahedron. By the symmetrical operation of $\bar{4}$, the "$\alpha - \gamma$" bond is equivalent to the "$\gamma - \beta$" bond, leading to an isosceles triangle composed of α, β, and γ. The Mn2 sites are similar in structure to the Mn1 sites, whereas the Mn3 sites form a zigzag chain. Another important feature is the short distances between the inequivalent Mn sites: 2.70 Å for

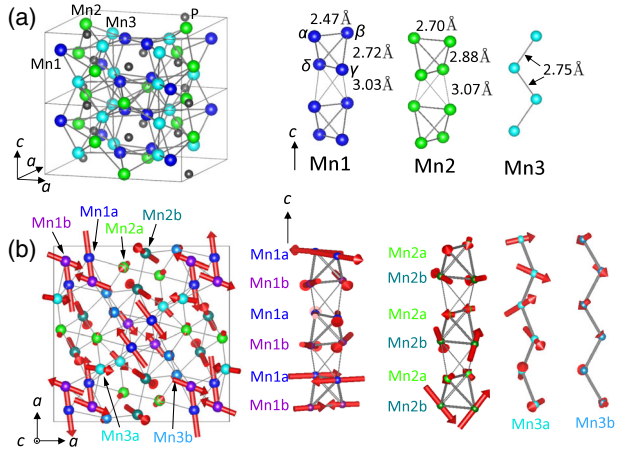

FIG. 1. (a) Crystal structure of noncentrosymmetric Mn_3P. Two unit cells are shown. Tetragonal structure of space group $I\bar{4}$ is composed of three Mn sites and one P site. The Mn1 and Mn2 sites form the tetrahedrons, while the Mn3 sites form the zigzag chain. (b) The helical magnetic structure of Mn_3P was determined at 7 K and at ambient pressure. Three Mn sites are separated into six sites with different modulations of their magnetic moments. Nearly AF couplings between the magnetic moments almost lying in the ab plane are seen at the Mn1a and Mn1b sites, respectively. The c-axis components are significant at the Mn2 and Mn3 sites.

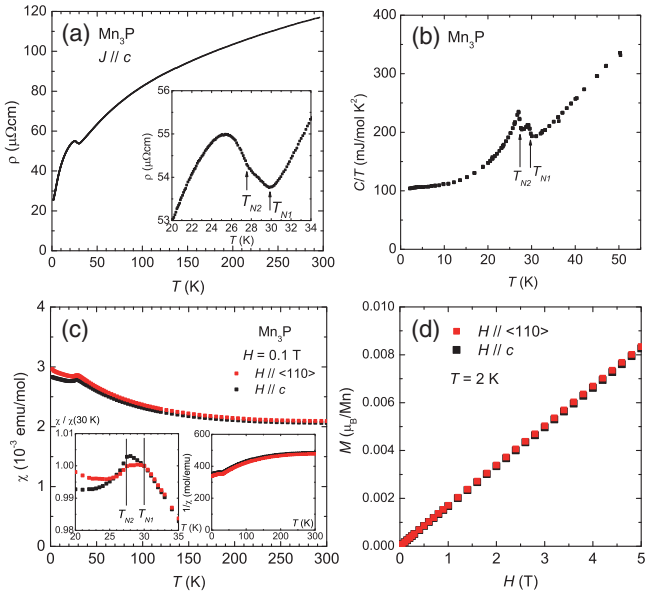

FIG. 2. Temperature dependence of (a) electrical resistivity, (b) T-divided specific heat (C/T), and (c) magnetic susceptibility at 0.1 T. All measurements detected two magnetic transitions: one at $T_{N1} = 30$ K, the other at $T_{N2} = 27.5$ K. The characteristic convex curve of ρ above T_{N1} is reminiscent of f-electron heavy fermion systems. (d) Magnetization curves at 2 K measured after field cooling.

Mn1-Mn2, 2.54 Å for Mn1-Mn3, and 2.55 Å for Mn2-Mn3. Fifteen different types of Mn-Mn bonds exist within 3.0 Å. Competition of the exchange interactions is expected among so many Mn-Mn bonds.

In this single-crystal study, we revealed that the itinerant antiferromagnet Mn_3P possesses unusual physical properties, such as a complex helimagnetic structure accompanied by a double transition and pressure-tuned quantum criticality accompanied by heavy-fermion-like behavior. The likely cause of these features is the frustration effect induced by the underlying structure.

Single crystals of Mn_3P were grown by the self-flux method, as described in the Supplemental Material [16]. We performed a range of experiments including resistivity, susceptibility, specific heat, neutron scattering, and NMR measurements. The resistivity and neutron scattering measurements were also conducted under pressure. We also calculated the band structure of Mn_3P. The experimental method, NMR results, and the band structure calculation are described in the Supplemental Material [16].

Figures 2(a)–2(c) plot the temperature dependences of (a) electrical resistivity (ρ), (b) T-divided specific heat (C/T), and (c) magnetic susceptibility (χ) of Mn_3P at ambient pressure. The ρ was characteristically convex below room temperature and exhibited two anomalies at $T_{N1} = 30$ K and $T_{N2} = 27.5$ K. The C/T demonstrated that both anomalies were second-order-like phase transitions. They were also confirmed by successive suppressions in χ. As shown in the magnetization curve after field cooling to 2 K [Fig. 2(d)], no spontaneous magnetization occurred in the ground state. Consistent with a previous report [14], the χ did not follow Curie-Weiss behavior [Fig. 2(c), inset], indicating the itinerant nature of the magnetism. The intrinsic nature of the double transition was further confirmed by NMR measurements [16], and the neutron scattering data shown below.

The magnetic structure of Mn_3P in the ground state was determined by neutron scattering measurements. The magnetic wave vector was found to be $\mathbf{Q} = (0.5, 0.5, \delta)$ with $\delta \sim 0.16$, which differs from the commensurate $\mathbf{Q}$ suggested in Ref. [14]. Figure 3(a) shows the temperature dependence of the scattering intensity at $\mathbf{Q} = (0.5, 2.5, 0.16)$. At ambient pressure, the intensity started increasing below T_{N1} and exhibited a small kink at T_{N2}, similarly to our NMR results [16]. The magnetic structure was refined using the 269 magnetic reflections measured at ambient pressure. We utilized two programs: the magnetic structure shown in Fig. 1(b) as given by Jana [22], and the modulations of the magnetic moment along the c axis given by Fullprof [23,24] and shown in Fig. 4. The resultant magnetic structures are consistent between the two programs. The crystal and magnetic-structure analyses are provided in the Supplemental Material [16]. In the ordered state shown in Fig. 1(b), each Mn site is split into two Mn sites with independently modulated amplitudes and phases. Mn1a and Mn1b (Mn2a and Mn2b) alternate along the c axis, and Mn3a and Mn3b form different zigzag chains. The complex noncollinear structure maintains a twofold rotational

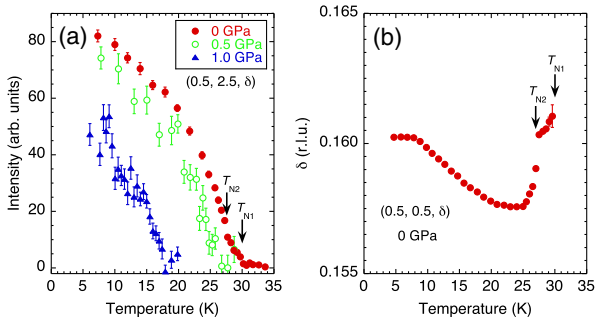

FIG. 3. (a) Temperature dependence of the magnetic Bragg intensities at (0.5, 2.5, δ) with $\delta \sim 0.16$, measured at different pressures. At ambient pressure, the magnetic scattering appears below T_{N1} and exhibits a small kink at T_{N2} (indicated by arrows). The two transitions are poorly resolved under pressure, but the scattering is observed at the same wave vector. (b) Temperature dependence of the incommensurability δ of the magnetic wave vector (0.5, 0.5, δ) at ambient pressure.

symmetry C_2. At most of the Mn sites, the size of the total magnetic moment oscillates along the c axis (see Fig. 4), indicating clear ellipticity of the helix. The origin of elliptical helices in d-electron systems is an interesting problem, and has been discussed in FeAs [25,26]. At all Mn sites, the size of the magnetic moment was about 1 μ_B or less, and was extremely small at the Mn2a and Mn3b sites. At the Mn1a and Mn1b sites, the magnetic moments almost presented in the ab plane, and were approximately coupled in antiparallel between the shortest "$\alpha - \beta$" (Mn1a) and the

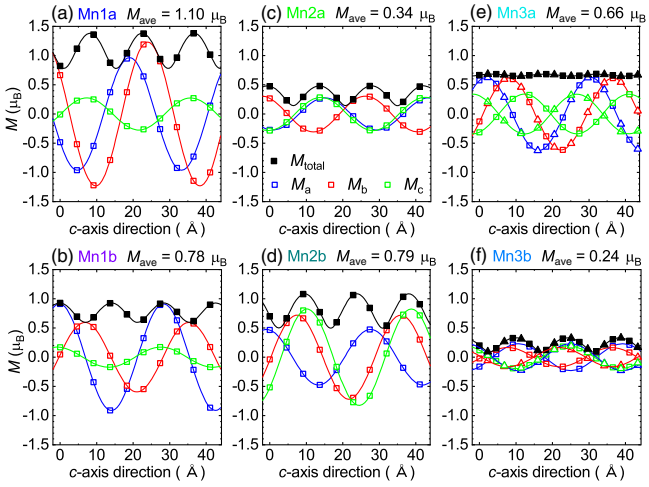

FIG. 4. Variation of the magnetic-moment components M_a, M_b, M_c, and M_{total}, along the c axis at six Mn sites, measured at 7 K under ambient pressure. M_{total} shows a clear ellipticity of the helix at most Mn sites. M_{ave} denotes the average value at each Mn site. At the Mn1a and Mn1b sites, the magnetic moments almost lie in the ab plane, but the moments are remarkably tilted at other sites. At the Mn3 sites, the squares and triangles indicate the two sublattices forming the zigzag chain. AF couplings between the sublattices appear in M_c ($M_{a,b}$) at the Mn3a (Mn3b) sites. The Fullprof refinement was obtained as $R_F = 11.3\%$.

"$\gamma - \delta$" (Mn1b) bonds owing to C_2 symmetry, indicating a dominance by AF exchange interactions. In the isosceles triangle composed of α, β, and γ, the AF interaction in the "$\alpha - \beta$" bond frustrates the equivalent interactions in the "$\beta - \gamma$" and "$\gamma - \alpha$" bonds, similarly to geometrical frustration. This yields a significant contribution to disturb the collinear magnetic ordering. At the Mn2 and Mn3 sites, the magnetic moments have substantial c-axis components. This helical state with the split sites, in which the sizes of the moments are significantly different, is conjectured to arise from reduced competition of the exchange interactions among the many Mn-Mn bonds. The contribution of the DM interaction is not clearly seen between the shortest Mn1-Mn1 bonds, which are almost coupled in antiparallel, but it will be important for reproducing the overall magnetic structure. At T_{N2}, the δ abruptly but continuously changed by ~2% [16]. The anisotropy of the averaged magnetic moment also changed when passing T_{N2} [16], but the weak magnetic intensities in the intermediate phase preclude a detailed analysis of the magnetic structure. We consider that the six Mn sites undergo partial ordering at T_{N1} and that the disordered Mn sites are ordered below T_{N2}.

The neutron scattering experiment clarified that all the Mn sites possess static magnetic moments, but the ordered states are unusual. At low temperatures, the C/T yielded a large electronic specific heat coefficient $\gamma = 104$ mJ/mol K^2, as shown in Fig. 2(b), corresponding to $\gamma_V = 3.6$ mJ/cm^3 K^2 per volume. This is one of the larger values in d electron systems [27]. The A coefficient of the T^2 term in the resistivity was also large value ($A = 0.52$ $\mu\Omega$ cm/K^2 at ambient pressure). The A/γ^2 ration was 4.8×10^{-5}, of the same order as the Kadowaki-Woods ratio. In the band calculation in the paramagnetic (PM) state [16], γ_{band} was estimated as 16.3 mJ/mol K^2 for a formula cell. The experimentally obtained γ in the ordered state was remarkably enhanced, suggesting that strong mass renormalization occurs in Mn_3P and survives even in the magnetically ordered state.

The pressure application drastically changed the electronic state of Mn_3P, as shown in Fig. 5(a). Both transitions (indicated by arrows) were quickly suppressed under pressure. The anomaly at T_{N2} disappeared above ~1.4 GPa, whereas T_{N1} tended to zero at 1.5–1.6 GPa. The residual resistivity decreased drastically to ~2 $\mu\Omega$ cm at ~1.6 GPa, and was thereafter independent of pressure. Obviously, the large residual resistivity ρ_0 is inherent in the ordered state, although its origin is unclear. The pressure-independent ρ_0 in the PM state probably originates from imperfectness in the sample, and its small value indicates a high-quality single crystal. Figure 6 shows the pressure-temperature phase diagram of Mn_3P, and the pressure dependences of ρ_0 and A. The continuous suppression of the ordered state suggests a quantum critical point (QCP) at $P_c \sim 1.6$ GPa. Among Mn-based systems, Mn_3P is a rare example of an easily inducible QCP; thus far, quantum phase transitions

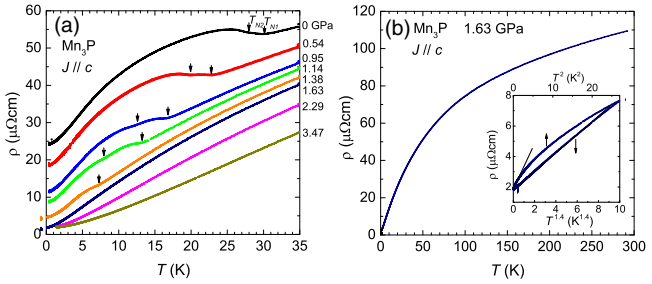

FIG. 5. (a) Electrical resistivity measured under pressure. The two transitions and the residual resistivity are simultaneously suppressed by applying pressure. (b) Resistivity behavior in the vicinity of the QCP. The residual resistivity ratio (RRR) is ∼58. The characteristic convexity appears over a wide temperature range. Inset: the resistivity at low temperature deviates from FL behavior, and obeys a $T^{1.4}$ dependence. The ρ vs T^2 plots at several pressures are shown in the Supplemental Material [16].

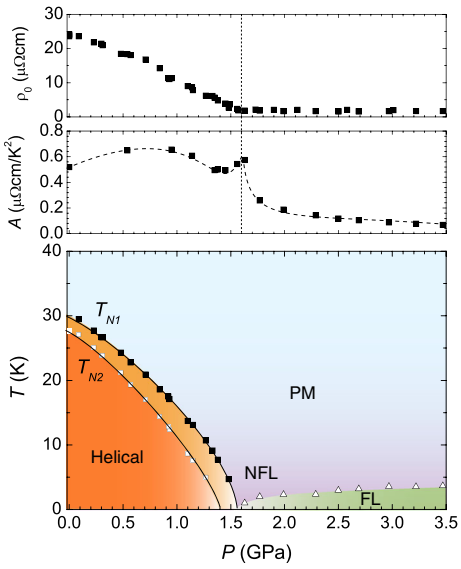

FIG. 6. Pressure dependences of ρ_0 and A coefficient, and pressure-temperature phase diagram of Mn_3P. In the vicinity of QCP, the NFL behavior is dominant. The A value is already large in the ordered state and shows a small peak at the QCP.

have been reported in only a few materials [28–30]. Another QCP, where T_{N2} reaches 0 K, is also expected at ∼1.4 GPa. The phase diagram suggests that two ordered phases are almost degenerate at any pressure. The pressure dependence of the magnetic Bragg intensities is shown in Fig. 3(a). The incommensurate structure with $\delta = 0.16$ was robust and no pressure dependence was observed up to 1 GPa; specifically, δ was 0.1608(2) at 0 GPa, 0.160(1) at 0.5 GPa, and 0.162(2) at 1 GPa. The ordered magnetic moment gradually reduced with increasing pressure, reaching ∼72% of its ambient-pressure value (on average) at 1 GPa.

Figure 5(b) plots the temperature dependence of resistivity at 1.63 GPa, just above P_c. The resistivity in the PM state was convex over a wide temperature range, reminiscent of f-electron heavy fermion systems. The resistivity remarkably decreased below 50–100 K, indicating a broad incoherent-coherent crossover in the low temperature region. As shown in the inset of Fig. 5(b), the resistivity at 1.63 GPa obeyed a $T^{1.4}$ dependence at low temperatures. The vicinity of the QCP was dominated by non-Fermi liquid (NFL) behavior and a distinct peak in the A, although A was already large in the ordered state. This indicates an unusually small entropy release through T_{N1} and T_{N2}. The A was suppressed at pressures above P_c, and the Fermi liquid (FL) state became stabilized. The observed A in Mn_3P (0.5–0.6 $\mu\Omega\,\mathrm{cm/K^2}$) is comparable to those of f-electron heavy fermion systems, and is ∼30 times larger than that of MnP, even near the QCP [30] where the helimagnetic phase terminates [31,32].

Several materials in d-electron systems have been reported as heavy fermion systems with strong mass renormalization. Examples are β-Mn, $(Y, Sc)Mn_2$, LiV_2O_4, $(Ca, Sr)RuO_4$, $Na_{1.5}Co_2O_4$, $CaCu_3Ir_4O_{12}$, and AFe_2As_2 (A = K, Cs) [33–40]. Such materials commonly exhibit a low characteristic temperature T^*, which generally gives a large γ proportional to $1/T^*$. Mn_3P should be included in this category. In the above oxides and iron pnictides, χ obeys Curie-Weiss behavior at temperatures above T^* [35,37–39,41], suggesting the presence of localized moments at high temperatures. Accordingly, T^* is generally interpreted as a localized-itinerant crossover, broadly analogous to that observed in the f-electron systems. The localized moment in d-electron systems primarily arises from proximity of a Mott insulator [41–44]. However, in Mn_3P, the deviation of χ from Curie-Weiss law and the band calculation [16] suggest the obvious itinerant character of the $3d$ electrons. It is unlikely that Mn_3P is compatible with models based on localized-itinerant crossover.

Heavy d-electrons may also arise from the effects of geometrical frustration, as discussed for β-Mn, $Y_{0.95}Sc_{0.05}Mn_2$ and LiV_2O_4. They are divided into models with localized moments [45–50] and itinerant models [51–53]. In the itinerant models, it has been proposed that frustration enhances the fluctuations of degenerate t_{2g} orbitals [52,53], but Mn_3P prohibits such degeneracy in principle, because the local symmetry of each Mn site is low as represented by its notation 1 (C_1). Another route to heavy mass is degeneracy of the magnetic correlations inherent in frustration [51]. This route may be qualitatively adapted to Mn_3P, which is not a geometrically frustrated lattice but exhibits the unusual features of a strong frustration effect, such as the almost-degenerated magnetic transitions and the splitting into six Mn sites with quite different magnetic moment. In contrast to other itinerant heavy-fermion systems, β-Mn and $Y_{0.95}Sc_{0.05}Mn_2$, Mn_3P is a clean system, which excludes the possibility that the disorder effect enhances the incoherency. The observed features in Mn_3P are worthy of further theoretical and experimental elucidations.

In conclusion, we performed comprehensive experimental characterizations and calculations of antiferromagnet Mn_3P. We first identified a complex helimagnetic structure, in which three Mn sites are separated into six sites of different sizes and directions of their magnetic moments. The helimagnetic structure accompanied by the double transition suggests competition of the exchange interactions, or frustration, in Mn_3P. Second, the QCP was easily induced under pressure, a rare behavior in Mn-based materials. Third, Mn_3P behaved similarly to f-electron-heavy fermion systems, namely, it presented a convex resistivity curve, a larger electronic specific heat coefficient than that estimated by the band-structure calculation, and a large A coefficient of the resistivity. They demonstrate a strong mass renormalization in Mn_3P. These noteworthy findings reveal that the itinerant system Mn_3P comprehends the areas of magnetism with competing interactions, a quantum criticality, and d-electron heavy fermion. It is an excellent example to merge them and to induce the novel interplay.

We thank Kazuto Akiba for experimental supports. This work was supported by JSPS KAKENHI Grants No. JP15H05882, No. JP15H05885, No. JP18H04320, and No. 18H04321 (J-Physics), No. 15H03689 and No. 15H05745. This research used resources at the High Flux Isotope Reactor and the Spallation Neutron Source, DOE Office of Science User Facilities operated by the Oak Ridge National Laboratory.

[1] H. v. Löhneysen, A. Rosch, M. Vojta, and P. Wölfle, Rev. Mod. Phys. **79**, 1015 (2007).
[2] P. Gegenwart, Q. Si, and F. Steglich, Nat. Phys. **4**, 186 (2008).
[3] T. Shibauchi, A. Carrington, and Y. Matsuda, Annu. Rev. Phys. Chem. **5**, 113 (2014).
[4] T. Furukawa, K. Miyagawa, H. Taniguchi, R. Kato, and K. Kanoda, Nat. Phys. **11**, 221 (2015).
[5] S. Takeuchi and K. Motizuki, J. Phys. Soc. Jpn. **24**, 742 (1968).
[6] A. Kallel, H. Boller, and E. F. Bertaut, J. Phys. Chem. Solids **35**, 1139 (1974).
[7] L. Dobrzynski and A. F. Andresen, J. Magn. Magn. Mater. **82**, 67 (1989).
[8] S. Yano, J. Akimitsu, S. Itoh, T. Yokoo, S. Satoh, D. Kawana, and Y. Endoh, J. Phys. Conf. Ser. **391**, 012113 (2012).
[9] T. Yamazaki, Y. Tabata, T. Waki, T. J. Sato, M. Matsuura, K. Ohoyama, M. Yokoyama, and H. Nakamura, J. Phys. Soc. Jpn. **83**, 054711 (2014).
[10] Y. Shiomi, S. Iguchi, and Y. Tokura, Phys. Rev. B **86**, 180404(R) (2012).
[11] S. Nakatsuji, N. Kiyohara, and Y. Higo, Nature (London) **527**, 212 (2015).
[12] T. Kurumaji, T. Nakajima, M. Hirschberger, A. Kikkawa, Y. Yamasaki, H. Sagayama, H. Nakao, Y. Taguchi, T. Arima, and Y. Tokura, Science **365**, 914 (2019).
[13] R. J. Gambino, T. R. McGuire, and Y. Nakamura, J. Appl. Phys. **38**, 1253 (1967).
[14] H.-p Liu, Y. Andersson, P. James, D. Satula, B. Kalska, L. Häggström, O. Eriksson, A. Broddefalk, and P. Nordblad, J. Magn. Magn. Mater. **256**, 117 (2003).
[15] S. Rundqvist, Acta Chem. Scand. **16**, 992 (1962).
[16] See the Supplemental Material at http://link.aps.org/supplemental/10.1103/PhysRevLett.124.087202, which contains the sample preparation, details of the experimental methods, the NMR spectrum, the band structure calculation, additional results and analyses of the neutron scattering measurement, and resistivity data under several pressures. It includes Refs. [17–21].
[17] G. M. Sheldrick, Acta Crystallogr. Sect. A **64**, 112 (2008).
[18] A. L. Spek, J. Appl. Crystallogr. **36**, 7 (2003).
[19] T. C. Kobayashi, H. Hidaka, H. Kotegawa, K. Fujiwara, and M. I. Eremets, Rev. Sci. Instrum. **78**, 023909 (2007).
[20] K. Murata, K. Yokogawa, H. Yoshino, S. Klotz, P. Munsch, A. Irizawa, M. Nishiyama, K. Iizuka, T. Nanba, T. Okada, Y. Shiraga, and S. Aoyama, Rev. Sci. Instrum. **79**, 085101 (2008).
[21] F. Ye, Y. Liu, R. Whitfield, R. Osborn, and S. Rosenkranz, J. Appl. Crystallogr. **51**, 315 (2018).
[22] V. Petricek, M. Dusek, and L. Palatinus, Z. Kristallogr. **229**, 345 (2014); V. Petricek *et al.*, Z. Kristallogr. Cryst. Mater. **231**, 301 (2016).
[23] J. Rodriguez-Carvajal, Physica (Amsterdam) **192B**, 55 (1993).
[24] https://www.ill.eu/sites/fullprof/.
[25] E. E. Rodriguez, C. Stock, K. L. Krycka, C. F. Majkrzak, P. Zajdel, K. Kirshenbaum, N. P. Butch, S. R. Saha, J. Paglione, and M. A. Green, Phys. Rev. B **83**, 134438 (2011).
[26] T. Frawley, R. Schoonmaker, S. H. Lee, C.-H. Du, P. Steadman, J. Strempfer, Kh. A. Ziq, S. J. Clark, T. Lancaster, and P. D. Hatton, Phys. Rev. B **95**, 064424 (2017).
[27] N. E. Hussey, J. Phys. Soc. Jpn. **74**, 1107 (2005).
[28] K. Takeda, A. Miyake, K. Shimizu, T. C. Kobayashi, and K. Amaya, J. Phys. Soc. Jpn. **77**, 025001 (2008).
[29] C. Pfleiderer, G. J. McMullan, and G. G. Lonzarich, Physica (Amsterdam) **206B&207B**, 847 (1995); C. Pfleiderer, S. R. Julian, and G. G. Lonzarich, Nature (London) **414**, 427 (2001).
[30] J.-G. Cheng, K. Matsubayashi, W. Wu, J. P. Sun, F. K. Lin, J. L. Luo, and Y. Uwatoko, Phys. Rev. Lett. **114**, 117001 (2015).
[31] M. Matsuda, F. Ye, S. E. Dissanayake, J.-G. Cheng, S. Chi, J. Ma, H. D. Zhou, J.-Q. Yan, S. Kasamatsu, O. Sugino, T. Kato, K. Matsubayashi, T. Okada, and Y. Uwatoko, Phys. Rev. B **93**, 100405(R) (2016).
[32] Y. Wang, Y. Feng, J.-G. Cheng, W. Wu, J. L. Luo, and T. F. Rosenbaum, Nat. Commun. **7**, 13037 (2016).
[33] T. Shinkoda, K. Kumagai, and K. Asayama, J. Phys. Soc. Jpn. **46**, 1754 (1979).
[34] M. Shiga, K. Fujisawa, and H. Wada, J. Phys. Soc. Jpn. **62**, 1329 (1993).
[35] S. Kondo, D. C. Johnston, C. A. Swenson, F. Borsa, A. V. Mahajan, L. L. Miller, T. Gu, A. I. Goldman, M. B. Maple, D. A. Gajewski, E. J. Freeman, N. R. Dilley, R. P. Dickey, J. Merrin, K. Kojima, G. M. Luke, Y. J. Uemura, O. Chmaissem, and J. D. Jorgensen, Phys. Rev. Lett. **78**, 3729 (1997).

[36] C. Urano, M. Nohara, S. Kondo, F. Sakai, H. Takagi, T. Shiraki, and T. Okubo, Phys. Rev. Lett. **85**, 1052 (2000).
[37] S. Nakatsuji, D. Hall, L. Balicas, Z. Fisk, K. Sugahara, M. Yoshioka, and Y. Maeno, Phys. Rev. Lett. **90**, 137202 (2003); S. Nakatsuji and Y. Maeno, Phys. Rev. B **62**, 6458 (2000).
[38] K. Miyoshi, E. Morikuni, K. Fujiwara, J. Takeuchi, and T. Hamasaki, Phys. Rev. B **69**, 132412 (2004).
[39] J.-G. Cheng, J.-S. Zhou, Y.-F Yang, H. D. Zhou, K. Matsubayashi, Y. Uwatoko, A. MacDonald, and J. B. Goodenough, Phys. Rev. Lett. **111**, 176403 (2013);
[40] Y. P. Wu, D. Zhao, A. F. Wang, N. Z. Wang, Z. J. Xiang, X. G. Luo, T. Wu, and X. H. Chen, Phys. Rev. Lett. **116**, 147001 (2016).
[41] F. Hardy, A. E. Böhmer, D. Aoki, P. Burger, T. Wolf, P. Schweiss, R. Heid, P. Adelmann, Y. X. Yao, G. Kotliar, J. Schmalian, and C. Meingast, Phys. Rev. Lett. **111**, 027002 (2013).
[42] R. Arita, K. Held, A. V. Lukoyanov, and V. I. Anisimov, Phys. Rev. Lett. **98**, 166402 (2007).
[43] P. E. Jönsson, K. Takenaka, S. Niitaka, T. Sasagawa, S. Sugai, and H. Takagi, Phys. Rev. Lett. **99**, 167402 (2007).
[44] V. I. Anisimov, I. A. Nekrasov, D. E. Kondakov, T. M. Rice, and M. Sigrist, Eur. Phys. J. B **25**, 191 (2002).
[45] P. Fulde, A. N. Yaresko, A. A. Zvyagin, and Y. Grin, Europhys. Lett. **54**, 779 (2001).
[46] C. Lacroix, Can. J. Phys. **79**, 1469 (2001).
[47] J. Hopkinson and P. Coleman, Phys. Rev. Lett. **89**, 267201 (2002).
[48] S. Burdin, D. R. Grempel, and A. Georges, Phys. Rev. B **66**, 045111 (2002).
[49] N. Shannon, Eur. Phys. J. B **27**, 527 (2002).
[50] M. S. Laad, L. Craco, and E. Müller-Hartmann, Phys. Rev. B **67**, 033105 (2003).
[51] C. Pinetts and C. Lacroix, J. Phys. Condens. Matter **6**, 10093 (1994).
[52] H. Tsunetsugu, J. Phys. Soc. Jpn. **71**, 1844 (2002).
[53] Y. Yamashita and K. Ueda, Phys. Rev. B **67**, 195107 (2003).